Dyes and Pigments 193 (2021) 109467

Contents lists available at ScienceDirect

Dyes and Pigments

journal homepage: www.elsevier.com/locate/dyepig

A red-emitting fluorescent probe imaging release of calcium ions from lysosome induced by chloroquine based on a photochromic crowned spirobenzopyran

Yingchun Wu [a,c], Caixia Yin [b,d], Weijie Zhang [b], Jianbin Chao [a], Fangjun Huo [a,c,*]

[a] Research Institute of Applied Chemistry, Shanxi University, Taiyuan, 030006, China
[b] Key Laboratory of Chemical Biology and Molecular Engineering of Ministry of Education, Institute of Molecular Science, Shanxi University, Taiyuan, 030006, China
[c] School of Chemistry and Chemical Engineering, Research Institute of Applied Chemistry, Shanxi University, Taiyuan, 030006, China
[d] Shanxi Laboratory for Yellow River, China

ARTICLE INFO

Keywords:
Calcium ion
Spiropyran
Chloroquine
Aza-15-crown-5

ABSTRACT

Calcium ions play an important role in intracellular signaling, metabolism and a wide range of cellular processes. An abnormal calcium concentration may cause many adverse symptoms, such as physiological responses in obesity, immune responses and pathological responses in Alzheimer's disease. Therefore, the development of specific fluorescent probes for monitor Ca^{2+} in living organism is of great significance. Herein, a red-emitting probe **SP-CE** was successfully designed and synthesized based on spiropyran derivatives as the fluorophore and aza-15-crown-5 as the sensing moiety for the recognition of calcium ions. Under the ultraviolet light irradiation, **SP-CE** was transformed to merocyanine (**MC**) form, which releasing negative oxygen ions, thereby achieving the recognition of calcium ions with the collaboration of crown ethers. According to the literature, chloroquine **(CQ)** could stimulate the up-regulation of pH in the sub-organelle lysosome in cells, resulting in changes of the calcium ions abundance in the cytoplasm. Interestingly, **SP-CE** could be used to visualize the occurrence of the above mentioned physiological processes in living cells. In addition, the probe **SP-CE** has been successfully employed for labeling calcium ions in living zebrafish model.

1. Introduction

Ca^{2+} plays a major role that transmits in intracellular signaling and a variety of intracellular processes [1–4]. However, dysregulation of intracellular Ca^{2+} signaling is related to physiological responses in obesity, immune responses and pathological responses in Alzheimer's disease [5–11]. Therefore, it is important to track the dynamic changes of calcium concentration in cytosolic and understand the Ca^{2+} signal pathways in cells [12]. In addition, according to the literature reported that chloroquine (**CQ**) could cause calcium ion release by increasing lysosomal pH. Importantly, blockading lysosomal calcium ions release disrupts **CQ**-induced M1 macrophages polarisation, suggesting that lysosomal calcium release is necessary [13]. Therefore, a specific and ultra-fast detection tool is urgently needed for visualizing the fluctuation of calcium ion abundance in living cells and in *vivo*, which is essential for preventing related diseases by formulating corresponding intervention strategies.

Fluorescent probes based on small organic molecules combined with fluorescence imaging technology, using their unique advantages of good specificity, high sensitivity, and in-situ monitoring, have become important research methods in modern life sciences and disease diagnosis [14–17]. To date, great efforts have been made to monitor metal ions based on crown ether recognition sites [18,19]. For example, Heng's research group designed a light-controllable spiropyran reversible sensor optical probe for calcium ion detection [20]. Subsequently, Yin's research group designed a fluorescent probe based on photochromic crown ether spiropyran for lithium ion detection [21]. However, these fluorescent probes for monitoring metal ions were rarely exploited at the level of cellular imaging.

Spiropyran (**SP**) is one of the most common photochromic compounds, under UV/visible light irradiation, which could be reversibly converted from **SP** form to **MC** form [22–24]. "Hard" metal ions could be chelated with crown ethers by using lone pairs from oxygen effectively [25]. Due to these favourable characteristics, we designed and

* Corresponding author. Research Institute of Applied Chemistry, Shanxi University, Taiyuan 030006, China.
E-mail address: huofj@sxu.edu.cn (F. Huo).

https://doi.org/10.1016/j.dyepig.2021.109467
Received 11 March 2021; Received in revised form 6 May 2021; Accepted 7 May 2021
Available online 2 June 2021

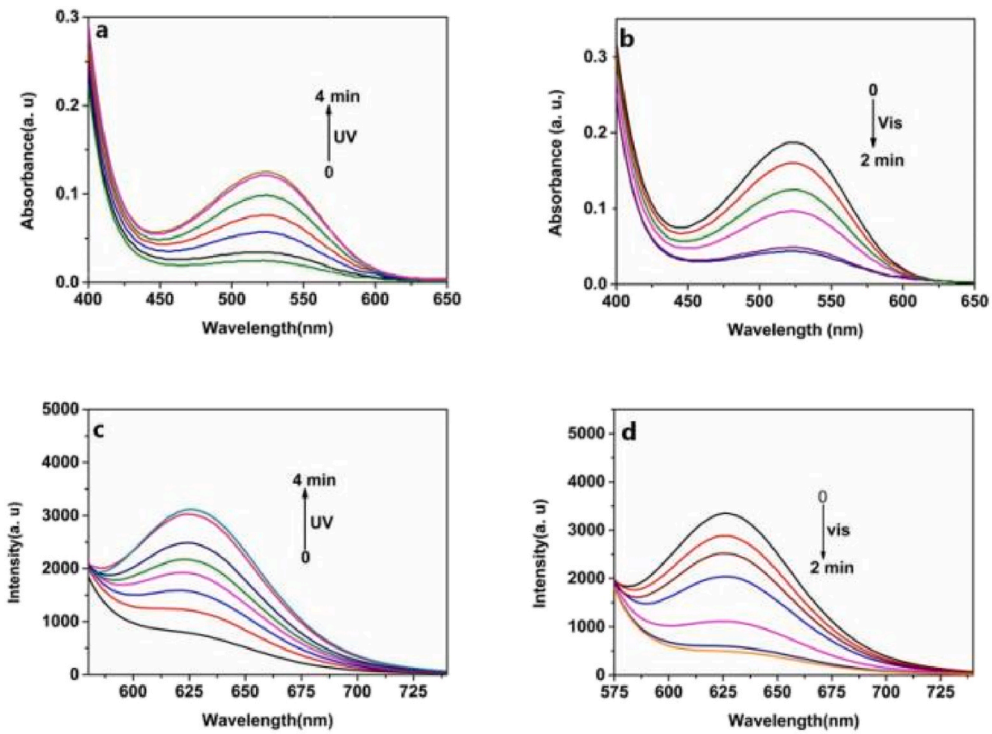

Fig. 1. Spectroscopic analysis of photochromic **SP-CE**. Fig. 1(a) and (b) show that the UV–Vis absorption spectrum change of **SP-CE** (0.1 mM) under the ultraviolet light irradiation and visible light irradiation in H_2O:CH_3CN = 4:1 (v/v). Fig. 1(c) and (d) shown the fluorescence spectral change of **SP-CE** (0.1 mM) under ultraviolet light irradiation and visible light irradiation.

synthesized a red-emitting fluorescent probe (**SP-CE**), using spiropyran derivatives as the fluorophore and aza-15-crown-5 as the recognition site for calcium ions. Upon adding calcium ions into H_2O:CH_3CN = 4:1 (v/v), the crown ether partly chelated with calcium ions to form corresponding complexe, and induced the hydroxyl in the **MC** to negative oxygen ions, which enhanced the coordination ability with calcium ions. Further cells and zebrafish experiments clearly revealed that **SP-CE** could be used to monitor calcium ions in biological systems. Additionally, the probe could detect the calcium ions released from lysosome to cytoplasm due to chloroquine-induced pH changes in the lysosome.

2. Experiments

2.1. Synthesis of SP-CE

2.1.1. Compound 1

Compound **1** was prepared according to literature [22]. mp, 176 °C–178 °C. IR (cm^{-1}): 3309, 2973, 2529, 1720, 1594, 1469, 1400, 1360, 1349, 1270, 1207, 1030, 939, 757. ESI-MS *m/z*: $[C + H]^+$ Calcd for $C_{14}H_{18}NO_2^+$ 232.13321, Found (Fig. S1).

2.1.2. Compound 2

Related synthetic steps for compound **2** were described in the support information.

2.1.3. Compound 3

Compound **2** (0.581 g, 1 mmol), EDCl (0.767 g, 4 mmol) and 1-hydroxybenzotriazole (0.54 g, 4 mmol) were dissolved in 15 mL of anhydrous N,*N*-dimethylformamide solution, the mixture was reacted for 30 min under the protection of argon at 0 °C. Then 1-aza-15-crown-5-ether (0.58 g, 1 mmol) and triethylamine (0.3 mL) were added to the reaction solution, and the mixture continued to react at room temperature for 24 h. After the reaction was completed, the reactants were poured into distilled water (100 mL) to continue stirring, and the resulting precipitate was filtered, washed with distilled water and dried in vacuum. Finally, a dark gray solid was obtained (0.30 g, 52.3%). A similar substance was reported in this patent. We referred to the synthesis method of **SP-CE** in this patent [26]. mp, 103 °C–106 °C. IR (cm^{-1}): 2970, 2865, 2362, 1706, 1641, 1609, 1508, 1484, 1460, 1331, 1270, 1126, 1081, 1029, 940, 912, 804, 747, 679.^{1}H NMR (600 MHz, CD_3CN) δ 8.10 (s, 1H), 8.03 (d, J = 8.9 Hz, 1H), 7.18 (t, J = 7.6 Hz, 1H), 7.14 (d, J = 7.2 Hz, 1H), 7.07 (d, J = 10.4 Hz, 1H), 6.86 (t, J = 7.4 Hz, 1H), 6.76 (d, J = 9.0 Hz, 1H), 6.68 (d, J = 7.7 Hz, 1H), 5.97 (d, J = 10.4 Hz, 1H), 3.66–3.34 (m, 22H), 2.72 (dt, J = 15.0, 7.4 Hz, 1H), 2.58–2.52 (m, 1H), 1.27 (s, 3H), 1.15 (s, 3H) (Fig. S3). ^{13}C NMR (151 MHz, CD3CN) δ 171.24, 159.32, 146.59, 141.14, 136.18, 128.10, 127.77, 125.64, 122.76, 122.01, 121.81, 119.41, 119.06, 115.37, 107.01, 106.83, 70.54, 70.44, 69.93, 69.75, 69.57, 69.49, 68.83, 52.56, 50.07, 48.67, 39.73, 31.65, 25.26, 18.95. ESI-MS of probe **SP-CE** *m/z*: $[SP\text{-}CE]^+$ calcd for 582.28129; $[SP\text{-}CE + Na]^+$ alcd for 604.26308 (Fig. S3).

2.2. Materials

Related solvents and apparatus are described in the support information.

2.3. Fluorescence imaging

2.3.1. Cell imaging

HeLa cells and HepG2 cells were cultured in DMEM medium containing 12% fetal bovine serum and 1% double antibody at 37 °C and 5% carbon dioxide incubator. When the cells were in the logarithmic growth phase, HeLa cells and HepG2 cells were inoculated in a special laser confocal culture dish, and continue culturing for another 24 h until the cells adhered to the wall.

The probe **SP-CE** (10 μM) was dissolved in phosphate buffered saline (PBS) (2 mL), and then added to a confocal culture dish inoculated with HeLa cells and HepG2 cells and incubated at 37 °C for 20 min. In the experiment for detecting exogenous calcium ions, the HeLa cells and HepG2 cells loaded with **SP-CE** were incubated in PBS at 37 °C for 20

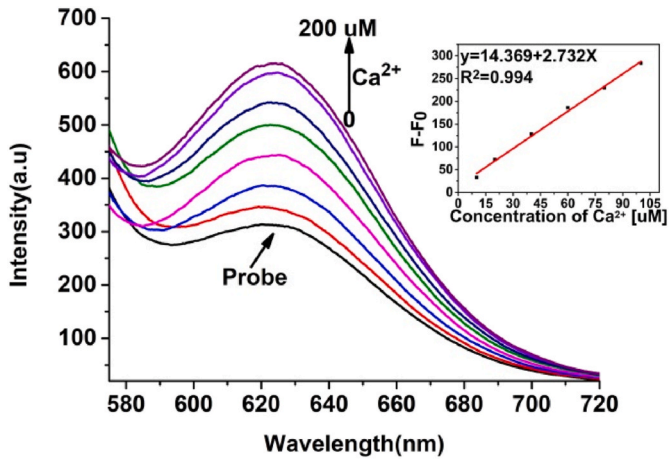

Fig. 2. Fluorescence spectrum responses of SP-CE (10 μM) to calcium ions (0–200 μM), in H_2O:CH_3CN = 4:1 (v/v) λ_{ex} = 535 nm, λ_{em} = 622 nm, slit: 10 nm/10 nm; Inserted: The working curve of **SP-CE** (10 μM) in the presence of various concentrations of Ca^{2+} (0–100 μM), λ_{ex} = 535 nm, slit: 10 nm/10 nm.

min, then incubated with calcium ions (100 μM) for 15 min, washed twice with PBS (2 mL), and then imaged. In the experiment for detecting endogenous calcium ions, HeLa cells and HepG2 cells loaded with **SP-CE** and **CQ** (100 μM) were incubated in PBS at 37 °C for 40 min, washed with PBS (2 mL) twice, and then imaged. The incubated cells were imaged under a UV lamp irradiation for 4 min.

2.3.2. Zebrafish culture and imaging

The probe **SP-CE** (20 μM) was added to E3 embryo medium containing zebrafish (5 days old) and incubated at 29 °C for 20 min and then imaged. In the experiment to detect exogenous calcium ions, the zebrafish was incubated with **SP-CE** (20 μM) for 20 min, then incubated with calcium ions (100 μM) for 20 min, then imaged. After incubation, the zebrafish was irradiated under UV light (365 nm) for 4 min.

3. Results and discussion

3.1. Study on the photochromic properties of probe SP-CE

We studied the photochromic properties of the **SP-CE**. The probe **SP-CE** (0.1 mM) showed a strong UV absorption band at 530 nm under the UV lamp 365 nm irradiation (0–4 min). However, when the **SP-CE** was irradiated with visible light (0–2 min), the UV absorption spectrum signal returned to the initial state, indicating that the **MC** form was converted into **SP** form. At the same time, when irradiated with 365 nm ultraviolet lamp, the fluorescence intensity of the **SP-CE** (0.1 mM) at 622 nm also increased with time (0–4 min). Nevertheless, it dropped to its original state under visible light irradiation, and the progress supported the UV–Vis spectrum analysis results.

3.2. SP-CE fluorescence spectrometric titration responds to calcium ions

The spectral properties of **SP-CE** and its response to calcium ions were obtained in H_2O:CH_3CN = 4:1 (v/v) (see Fig. 1). Upon adding (0–200 μM) calcium ions to the detection solution containing probe **SP-CE** (10 μM), the solution changed from light pink to dark pink and the corresponding spectrum mainly showed an upward trend at near 620 nm, as depicted in Fig. 2. We plotted the maximum emission intensity of **SP-CE** at λ_{ex} = 535 as a function of calcium ions concentration. The probe exhibited a good linear range and low detection limit (0.570 μM) for calcium ions (0–100 μM) (Fig. 2 Inserted). The detection limit of the probe was calculated according to the definition of IUPAC (CDL = 3σ/k) [27,28].

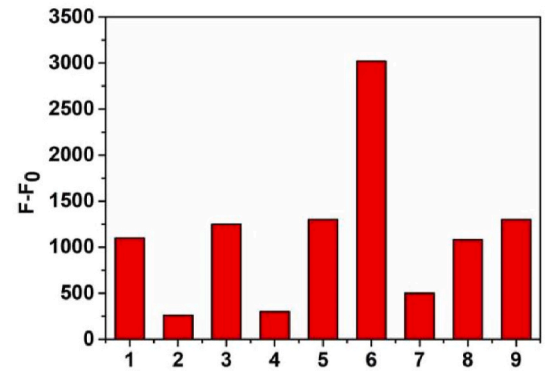

Fig. 3. Fluorescence response of probe **SP-CE** (100 μM) towards various biologically relevant species (500 μM) at 622 nm, (1) Zn^{2+} (2) Cu^{2+}, (3) Na^+, (4) Ag^+, (5) Mg^{2+}, (6) Ca^{2+}, (7) Fe^{2+}, (8) Li^+, (9) K^+.

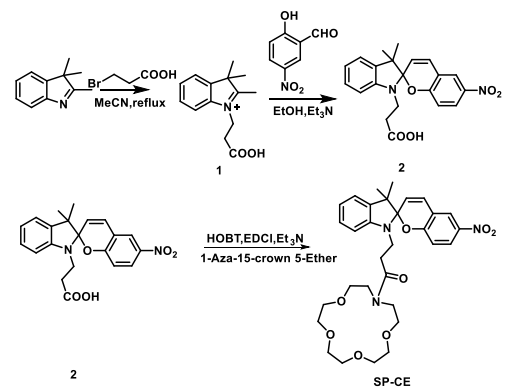

Scheme 1. Synthesis route for **SP-CE**.

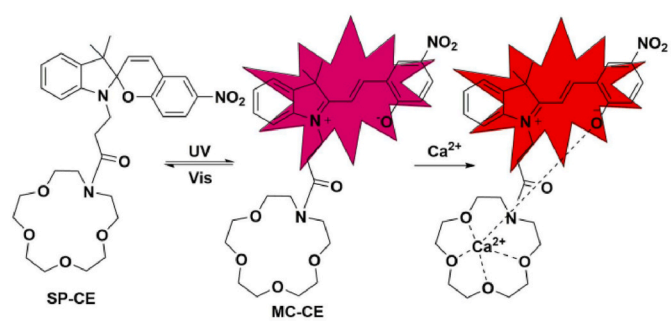

Scheme 2. Mechanism diagram of the **SP-CE** response Ca^{2+}.

3.3. Selectivity of SP-CE

We then tested the selection recognition of the **SP-CE** to calcium ions under H_2O:CH_3CN = 4:1 (v/v). As shown in Fig. 3, after adding calcium ions, the emission intensity increased significantly at 622 nm. Whereas upon the addition of other ions (500 μM) (Zn^{2+}, Cu^{2+}, Na^+, Ag^+, Mg^{2+}, Fe^{2+}, Li^+, K^+), the emission intensity did not increase remarkably. Therefore, the experiment proved that **SP-CE** has good selectivity to calcium ions. In addition, We tested the effect of different pH on the fluorescence responses of **SP-CE** to calcium ions. Notably, the fluorescence changes of **SP-CE** to Ca^{2+} reached a maximum at around pH = 7. It was further confirmed that **SP-CE** could recognize Ca^{2+} in physiological environment (Fig. S5).

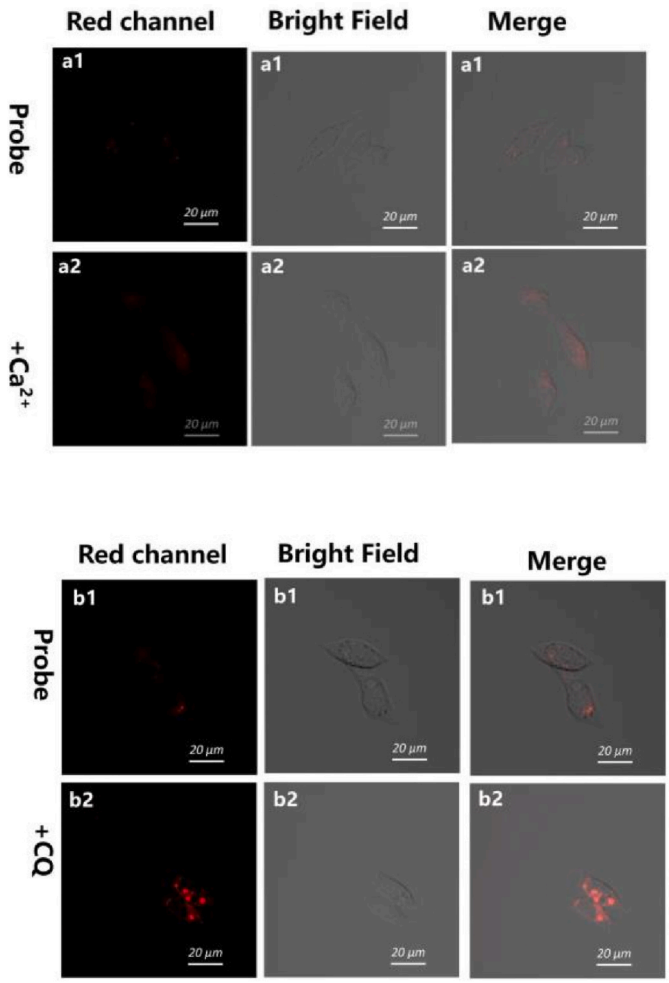

Fig. 4. Confocal images of the **SP-CE** responds to exogenous $Ca^{2+}$and endogenous Ca^{2+} in HepG2 cells. (a1) HepG2 cells were incubated with **SP-CE** (10 μM) for 20 min (a2) HepG2 cells were incubated with **SP-CE** (10 μM) for 20 min, and then incubated with exogenous calcium ions (0.1 mM) for 15 min (b1) HepG2 cells were incubated with **SP-CE** (10 μM) for 20 min (b2) HepG2 cells were incubated with **SP-CE** (10 μM) and CQ (100 μM) for 40 min. Red channel: emission wavelength 622 ± 20 nm (excitation wavelength 535 nm) Scale bar: 20 μM.

3.4. Proposed mechanism

The response mechanism of **SP-CE** for detecting calcium ions was described in Scheme 2. Besides, as shown in Scheme 2, the SP-CE structure was easily transformed into MC-CE structure under UV irradiation, and the presence of calcium ions would further promoted the transformation of SP-CE structure into MC-CE through the combined action of negative oxygen anions and crown ether. Therefore, the fluorescence intensity was significantly enhanced after adding calcium ions. The corresponding reaction product was characterized by **ESI-MS**. The **SP-CE** acetonitrile solution (1 mL, 1 mM) was mixed with $CaCl_2$ aqueous solution under the ultraviolet light irradiation for 4 min, and then sample were measured by a mass spectrometer. As shown in Fig. S4, an obvious strong peak indicates that **MC-CE** is stably complexed with calcium ions. Due to the influence of the negative oxygen ion of spiropyran on the binding efficiency of calcium ions, we used Prism-8 software to perform a non-linear regression fitting for calcium ions, as shown in Fig. S6, the stability constant of the **SP-CE** combining with calcium ions was 1.12×10^4 M^{-1} in H_2O: CH_3CN = 4:1. Therefore, the selective binding of **MC-CE** isomer for calcium ions was attributed to the electrostatic interaction with *p*-nitrophenolate and the suitability of the size of alkali metal ions and crown ethers. (see Scheme 1)

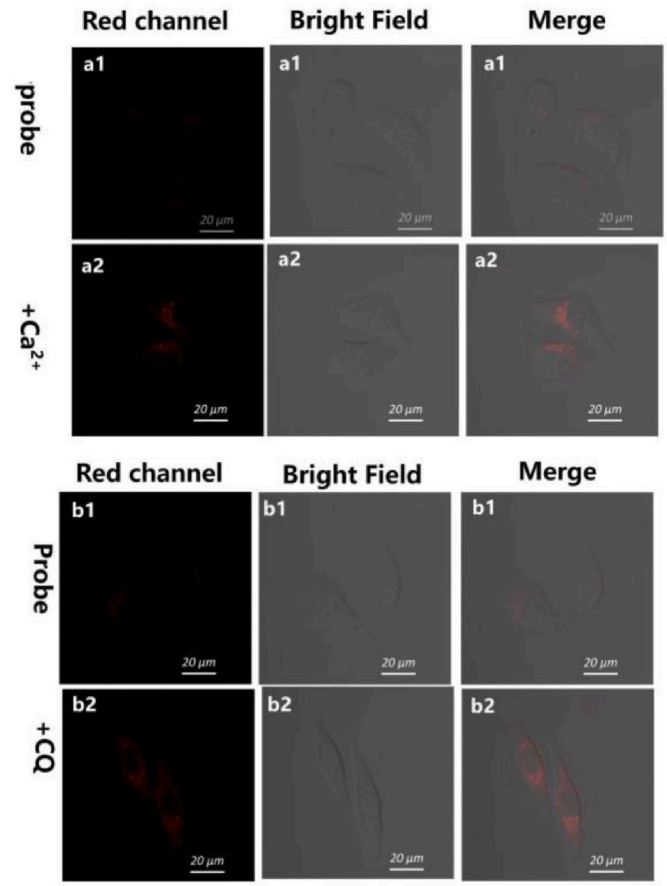

Fig. 5. Confocal images of the **SP-CE** responds to exogenous $Ca^{2+}$and endogenous Ca^{2+} in HeLa cells. (a1) HeLa cells were incubated with probe **SP-CE** (10 μM) for 20 min (a2) HeLa cells were incubated with **SP-CE** (10 μM) for 20 min, then treated with exogenous calcium ions (0.1 mM) for 15 min (b1) HeLa cells were incubated with **SP-CE** (10 μM) for 20 min (b2) Hela cells were incubated with **SP-CE** (10 μM) and CQ (100 μM) for 40 min. Red channel: emission wavelength 622 ± 20 nm (excitation wavelength 535 nm) Scale bar: 20 μM.

3.5. Cellular imaging

We evaluated the **SP-CE** response to calcium ions in cell imaging experiments. After HepG 2 cells with **SP-CE** (10 μM) were incubated for 20 min and then irradiated with UV light (4 min), a weak red fluorescence signal appeared in the red channel (Fig. 4a1). Furthermore, we also tracked to the exogenous calcium ions by fluorescence imaging. HepG2 cells were incubated with **SP-CE** (10 μM) for 20 min and then incubated with calcium ions (0.1 mM) for 15 min and irradiated with UV light (4 min). A similar fluorescence phenomenon appeared in the red fluorescence signal, and it was greatly enhanced. (Fig. 4a2). Meanwhile, we also investigated the sensing performance of probe **SP-CE** for endogenous calcium ions in living cells. We used **CQ** drugs that change the lysosomal pH value, causing calcium ions to be released into the cytoplasm. As shown in Fig. 4b2, HepG2 cells were cultured with the **SP-CE** (10 μM) and **CQ** (100 μM) for 40 min, a significant red fluorescence signal was enhanced in the red fluorescence channel. At the same time, **SP-CE** was studied in HeLa cells (Fig. 5). These results implied that **SP-CE** could be considered as a cell-permeable molecular tool to examine and visualize dynamic equilibrium of calcium ions in cells.

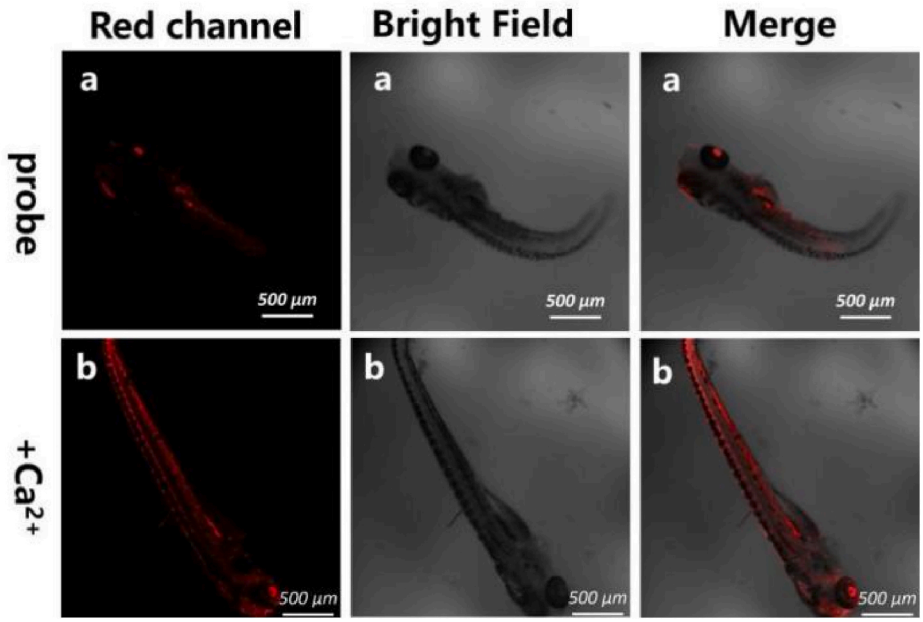

Fig. 6. Confocal images of probe **SP-CE** response to exogenous Ca^{2+} in zebrafish. (a) The zebrafish was incubated with the **SP-CE** (20 μM) for 20 min, and then irradiated with UV (365 nm) light for 4 min. (b) The **SP-CE**-loaded (20 μM) zebrafish incubated for 20 min then incubated with Ca^{2+} (100 μM) for 20 min, and then irradiated with UV (365 nm) light for 4 min. Red channel: emission wavelength 622 ± 20 nm (excitation wavelength 535 nm) Scale bar: 500 μM.

3.6. Zebrafish imaging

Next, we explored the feasibility of using the probe **SP-CE** (20 μM) for imaging low concentration of calcium in zebrafish. As shown in Fig. 6a, the zebrafish was incubated with the probe **SP-CE** (20 μM) for 20 min and then irradiated with UV lamp at 365 nm for 4 min, a weak red fluorescence signal appeared in the red channel. Simultaneously, when the zebrafish was incubated with **SP-CE** (20 μM) for 20 min, then incubated with calcium ions (100 μM) for 20 min, under the ultraviolet light irradiation for 4 min, the red fluorescence signal was enhanced in the red channel (Fig. 6b). Therefore, these imaging findings demonstrate the probe can effectively image calcium ions in vivo.

4. Conclusions

In summary, a red-emitting fluorescent probe **SP-CE** was explored to detect the endogenous and exogenous calcium ions in cells. **SP-CE** response mechanism was based on calcium ion induce the isomerized spiropyran **MC** to release negative oxygen ions, which could be specifically combined with crown ethers to achieve specific detection for calcium ions. Besides, further cells and zebrafish experiments clearly revealed that **SP-CE** could be used for monitoring calcium ions in biological system. Moreover, we applied **CQ** drugs to promote the release of calcium ions into the cytoplasm and to detect the level of calcium ion in the cytoplasm.

Declaration of competing interest

The authors declare that they have no known competing financial interests or personal relationships that could have appeared to influence the work reported in this paper.

Acknowledgments

We thank the National Natural Science Foundation of China (No. 21775096, 21907062), One hundred people plan of Shanxi Province, Shanxi Province"1331 project" key innovation team construction plan cultivation team (2018-CT-1), 2018 Xiangyuan County Solid Waste Comprehensive Utilization Science and Technology Project (2018XYSDJS-05), the Shanxi Province Foundation for Selected (2019), Key R&D Program of Shanxi Province (201903D421069), Natural Science Foundation of Shanxi Province of China (201901D111015), Shanxi Province Foundation for Returness (2017–026), Teaching reform project of colleges and universities in Shanxi Province (2019), Innovative Talents of Higher Education Institutions of Shanxi (2019), Scientific and Technological Innovation Programs of Higher Education Institutions in Shanxi (2019L0031), Shanxi Collaborative Innovation Center of High Value-added Utilization of Coal-related Wastes (2015-10-B3) and Scientific Instrument Center of Shanxi University (201512).

Appendix A. Supplementary data

Supplementary data to this article can be found online at https://doi.org/10.1016/j.dyepig.2021.109467.

Author contributions

Yingchun Wu: Investigation.
Fangjun Huo: Conceptualization, Writing-original draft.
Weijie Zhang: Validation.
Jianbin Chao: Project administration.
Caixia Yin: Funding acquisition, Writing-review & editing.

Declaration of interest statement

We have no any interest conflict.

References

[1] Fedrizzi L, Lim D, Carafoli E. Calcium and signal transduction. Biochem Mol Biol Educ 2008;36:175–80.
[2] Scharff O, Foder B. Regulation of cytosolic calcium in blood cells. Physiol Rev 1993;73:547–82.
[3] Komatsu H, Miki T, Citterio D. Single molecular multianalyte (Ca^{2+}, Mg^{2+}) fluorescent probe and applications to bioimaging. J Am Chem Soc 2005;127:10798–9.
[4] Berridge MJ, Bootman MD, Roderick HL. Calcium signalling: dynamics, homeostasis and remodeling. Nat Rev Mol Cell Biol 2003;4:517–29.

[5] LaFerla FM. Calcium dyshomeostasis and intracellular signalling in alzheimer's disease. Nat Rev Neurosci 2002;3:862–72.
[6] Grynkiewicz G, Poenie M, Tsien RY. A new generation of Ca^{2+} indicators with greatly improved fluorescence properties. Biol Chem 1985;260:3440–50.
[7] Harootunian AT, Kao JPY, Paranjipe S, Tsien RY. Genration of calcium oscillations in fibroblasts by positive feedback between calcium and IP3. Science 1991;251:75–8.
[8] Chambers J, Ames RS, Bergsma D. Melanin-concentrating hormone is the cognate ligand for the orphan G-protein-coupled receptor SLC-1. Nature 1999;400:261–5.
[9] Micu I, Ridsdale A, Zhang LQ. Real-time measurement of free Ca^{2+} changes in CNS myelin by two-photon microscopy. Nat Med 2007;13:874–9.
[10] Skokos D, Shakhar G, Varma R, Waite JC. Peptide-MHC potency governs dynamic interactions between T cells and dendritic cells in lymph nodes. Nat Immunol 2007;8:835–44.
[11] Kuchibhotla KV, Lattarulo CR, Hyman BT. Astrocytes in alzheimer's. Sci Signal 2009;323:1211–5.
[12] Minta A, Kao J, Tsien RY. Fluorescent indicators for cytosolic calcium based on rhodamine and fluorescein chromophores. J Biol Chem 1989;264:8171–8.
[13] Chen DG, Xie J, Fiskesund R. Chloroquine modulates antitumor immune response by resetting tumor-associated macrophages toward M1 phenotype. Nat Commun 2018;9:873.
[14] Xing M, Wang K, Wu X, Ma S, Cao D, Guan R, Liu Z. A coumarin chalcone ratiometric fluorescent probe for hydrazine based on deprotection, addition and subsequent cyclization mechanism. Chem Commun 2019;55:14980.
[15] Cao D, Liu Z, Verwilst P, Koo S, Jangjili P, Kim J, Lin W. Coumarin-Based small-molecule fluorescent chemosensors. Chem Rev 2019;119:10403.
[16] Niu L, Guan Y, Chen Y, Wu L, Tung C, Yang Q. BODIPY-Based ratiometric fluorescent sensor for highly selective detection of glutathione over cysteine and homocysteine. J Am Chem Soc 2012;134:18928.
[17] Liu Y, Ren DD, Zhang JJ, Li H, Yang XF. A fluorescent probe for hydrazine based on a newly developed 1-indanone-fused coumarin scaffold. Dyes Pigments 2019;162:112–9.
[18] Rurack K, Kollmannsberger M, Daub J. A selective and sensitive fluoroionophore for Hg (II), Ag (I), and Cu (II) with virtually decoupled fluorophore and receptor units. J Am Chem Soc 2000;122:968–9.
[19] Kim HM, Jeong MY, Ahn HC. Two-photon sensor for metal ions derived from azacrown ether. J Org Chem 2004;69:5749–51.
[20] Heng S, Mak AM, Kostecki R. Photoswitchable calcium sensor: 'On'–'Off' sensing in cells or with microstructured optical fibers. Sensor Actuator B Chem 2017;252:965–72.
[21] Yin CX, Li EZ, Kang J. A prospective material for the highly selective extraction of lithium ions based on a photochromic crowned spirobenzopyran. J Mater Chem B 2019;7:903–7.
[22] Zhang WJ, Huo FJ, Yin CX. Photocontrolled single-/dual-Site alternative fluorescence probes distinguishing detection of H_2S/SO_2 in vivo. Org Lett 2019;21:5277–80.
[23] Zhu JJ, Gao Q, Tong QX, Wu GF. Fluorescent probes based on benzothiazole-spiropyran derivatives for pH monitoring in vitro and in vivo. Spectrochim Acta A 2020;225:117506.
[24] Zhang WJ, Huo FJ, Yue YK. Heat stroke in cell tissues related to sulfur dioxide level is precisely monitored by light-controlled fluorescent probes. J Am Chem Soc 2020;142:3262–8.
[25] Kataky R, Nicholson PE, Parker D, Covington AK. Comparative performance of 14-crown-4 derivatives as lithium-selective electrodes. Analyst 1991;116:135–40.
[26] Sasaki H, Ito Y, Kawashima K, Mitsuya T and Hoshi N, Reusable printing plate containing photochromic latent image-forming substance, manufacture of printing plate, and printing apparatus using the same, Japanese Patent 2002274075.
[27] Zhang WJ, Liu T, Huo FJ, Ning P. Reversible ratiometric fluorescent probe for sensing bisulfate/H_2O_2 and its application in zebrafish. Anal Chem 2017;89:8079–83.
[28] Zhang WJ, Huo FJ, Liu T. Ratiometric fluorescence probe for hydrazine vapor detection and biological imaging. J Mater Chem B 2018;6:8085–9.